

Strain- and overlayer-induced in-plane magnetocrystalline anisotropy: First-principles determination for fcc (110) Co thin films

Miyoung Kim, Lieping Zhong, and A. J. Freeman

Department of Physics and Astronomy, Northwestern University, Evanston, Illinois 60208-3112

(Received 11 August 1997)

The in-plane interface magnetocrystalline anisotropy (MCA) of fcc Co (110), either as a free standing monolayer or as an overlayer on a Cu substrate, is investigated using the local density all-electron full-potential linearized augmented plane-wave method. We find an in-plane MCA which has the same order of magnitude as the perpendicular MCA, and which exhibits a significant twofold anisotropy. The results for free standing monolayers calculated with different lattice constants reveal that (i) the strength of the in-plane MCA is severely changed by the strain — introducing an 8% strain (relative to the Cu lattice constant) induces a five times larger in-plane MCA — and (ii) the change of band structure due to the strain plays an important role in determining the in-plane MCA. The strength of the in-plane MCA is found to be largely enhanced by the nonmagnetic Cu substrate while it is reduced by the structural relaxation. Interestingly, for all systems the in-plane easy axis is found to lie along $[\bar{1}10]$, which is along the direction of the in-plane nearest neighbor atom. [S0163-1829(98)01710-X]

Interface magnetocrystalline anisotropy (MCA) continues to be one of the most interesting topics in magnetism, not only because of its potential application for high-density magneto-optical storage media but also because determining its underlying driving mechanism is important for understanding the basic static properties of magnetic systems. Today, most of this research is devoted to systems that display magnetic orientations perpendicular to the surface. One important system is Co films on nonmagnetic transition metal substrates,¹ for which, in addition to perpendicular interface anisotropy, an in-plane anisotropy was found and investigated in order to achieve a better understanding of the nature of MCA. Recently, this in-plane MCA has drawn great interest due to experiments on reduced symmetry surfaces consisting of steps which include the lower-order in-plane anisotropy contribution.² It also provides a severe challenge to modern first principles theory.

For the (001) surface of a cubic material which has fourfold rotational symmetry about the film normal, the phenomenological expression for the interface anisotropy energy is given by

$$E_{sl} = E_z^{(2)}\alpha_z^2 + E_{xz}^{(4)}(\alpha_x^2\alpha_z^2 + \alpha_y^2\alpha_z^2) + E_{xy}^{(4)}\alpha_x^2\alpha_y^2 + \mathcal{O}(\alpha^6) \\ \approx K^{(2)}\cos^2(\theta) + K^{(4)}\sin^4(\theta)\cos(4\phi) \quad (1)$$

provided that higher order corrections can be ignored. Here $\alpha_x, \alpha_y,$ and α_z are the direction cosines of the magnetic moment with respect to the $\hat{x}, \hat{y},$ and \hat{z} axes and ϕ and θ are the polar angles measured from the \hat{x} and \hat{z} axes, respectively. The $\cos^2(\theta)$ term in Eq. (1) comes from the second order direction cosines and depends only on θ : the ϕ dependence is included in the fourth order term that exhibits a fourfold in-plane symmetry. Provided that this fourth order term is negligible compared to the second order term, the MCA will be given by a function of θ only — as assumed in

most of the MCA calculations which take ϕ to be zero so as to save on computational effort.

For a surface with a lower rotational symmetry about the film normal, however, the leading order terms in ϕ and θ are comparable and so the MCA must be considered as a function of ϕ as well as θ . For example, in the case of the (110) surface of cubic symmetry where the $\alpha_x\alpha_y$ term is not forbidden by twofold rotational symmetry on the surface, the phenomenological interface anisotropy energy must have the form

$$E_{sl} \approx K_1^{(2)}\cos^2(\theta) + K_2^{(2)}\sin^2(\theta)\cos^2(\phi) \quad (2)$$

when keeping the lowest order terms.³ Since the anisotropy constants $K_1^{(2)}$ and $K_2^{(2)}$ come from the same (second) order, the $K_2^{(2)}$ term (which gives the in-plane dependence of MCA) may no longer be negligible and hence should be considered. This term implies a twofold in-plane anisotropy.

In fact, the fourfold in-plane anisotropy of the (001) oriented surface was found to be much smaller compared to the perpendicular anisotropy — experimentally for bcc Fe and fcc Co thin films⁴ and computationally for several transition metal monolayers (ML)⁵. In contrast, a strong twofold in-plane MCA was observed experimentally for Fe (110) films on a W(110) substrate with an in-plane surface anisotropy constant that is 61% of the perpendicular anisotropy constant.⁶ However, there have been few theoretical works on the in-plane MCA other than tight-binding model calculations, which also reported a significant in-plane anisotropy of (110) surfaces.⁷⁻⁹

In this paper, we present results of first principles calculations of the in-plane MCA for fcc (110) Co as a free standing monolayer and as an overlayer on a Cu substrate. The overlayer case is simulated by a five layer Cu slab covered by a layer of Co on each side of the slab placed at the ideal fcc sites. Structural relaxation was accomplished by optimizing the vertical positions of all atoms utilizing the atomic

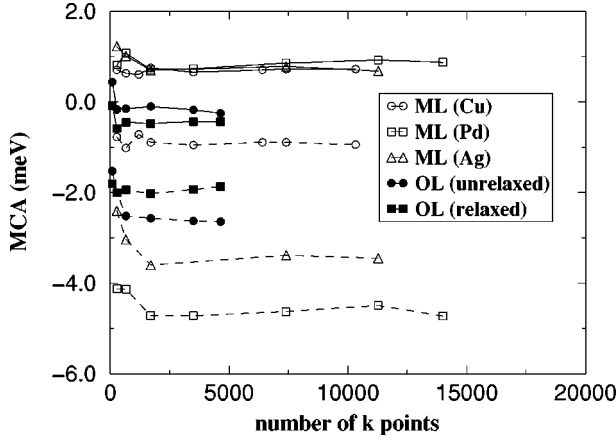


FIG. 1. Convergence of the MCA as a function of the number of k points in the full 2D BZ for fcc Co thin films in (110) orientation for free monolayers (ML) with Cu (open circles), Pd (open squares), and Ag (triangles) lattice constants and for unrelaxed (filled circles) and relaxed (filled squares) Co overlayers (OL) on Cu (110). The solid and dashed lines are for $K_2^{(2)}$ and $K_1^{(2)}$, respectively.

force approach.¹⁰ In order to isolate possible strain effects induced by Co epitaxy on different substrates, we study the free standing ML with three different lattice constants, i.e., those corresponding to Cu, Pd, and Ag ($a = 4.83, 5.20,$ and 5.47 a.u.) where the latter two introduce a strain of 8 and 13 % of the Cu lattice constant.

We used the full-potential linearized-augmented-plane wave (FLAPW) method¹¹ within the local spin density approximation, in which the core states are treated fully relativistically and the valence states are treated semirelativistically, i.e., without spin-orbit coupling (SOC)¹². To obtain the self-consistent scalar relativistic charge density and potential, we used 100 k points in the 2D irreducible Brillouin zone (IBZ). Within the muffin-tin (MT) spheres, lattice harmonics with angular momentum l up to 8 are used to expand the charge density, potential and wave functions. The SOC Hamiltonian matrix elements are calculated by integrating the derivative of the spherical potential over the MT regions and are treated in a second variational manner.¹³ Employing an increased number of k points, which corresponds to around 2 to 3×10^3 k points in the full BZ depending on the system (see, Fig. 1), provides less than a 10% fluctuation of the MCA value itself. We adopt the state tracking method¹⁴ to determine the new SOC induced occupied states which, as can be seen from Fig. 1, efficiently reduces the fluctuation of the MCA with a small number of k points compared to other methods.^{1,5}

The interface MCA, ΔE_{sl} , is determined by calculating the torque which is defined as the partial derivative of the anisotropy energy with respect to θ .¹⁵ Usually, the MCA is defined by the difference in the total energy of the magnetic moment oriented in-plane and oriented perpendicular to the surface. Even in case of the MCA dependence on ϕ , this is equivalent to calculating the torque at $\theta=45^\circ$ since from Eq. (2)

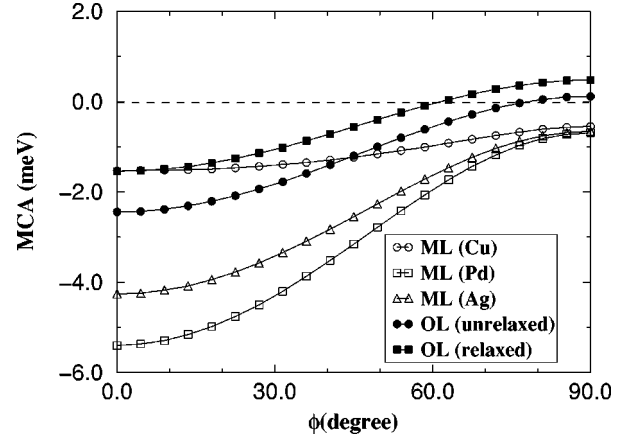


FIG. 2. The calculated in-plane angular dependence of MCA as a function of ϕ for the free Co ML and for Co on Cu (110), using the same notation for the data points of each system as in Fig. 1.

$$T(\theta=45^\circ, \phi) \equiv \left[\frac{\partial E_{sl}(\theta, \phi)}{\partial \theta} \right]_{\theta=45^\circ} = -K_1^{(2)} + K_2^{(2)} \cos^2(\phi) \\ = E_{sl}(\theta=90^\circ, \phi) - E_{sl}(\theta=0^\circ) \equiv \Delta E_{sl}. \quad (3)$$

Hence, according to this analysis, the MCA was determined by calculating the torque at $\theta=45^\circ$ as a function of ϕ . We take \hat{z} as the plane normal $[110]$ direction and \hat{x} as the direction of the nearest neighbor atom in the x - y plane, $[\bar{1}10]$, from which ϕ is measured.

The MCA calculated for the free Co ML with different lattice constants and for the Co overlayer on Cu (110) are plotted in Fig. 2 as a function of ϕ . All systems exhibit qualitatively the same behavior for the in-plane dependence of MCA: the MCA shows a significant twofold in-plane anisotropy that is well fitted by a $-K_1^{(2)} + K_2^{(2)} \cos^2(\phi)$ function with its easy axis along $[\bar{1}10]$ which is the direction of the nearest neighbor atom in the x - y plane. The anisotropy constants $K_1^{(2)}$ and $K_2^{(2)}$ determined by the fitting are given in Table I. Clearly, the strength of the in-plane MCA ($K_2^{(2)}$) is the same order of magnitude as the perpendicular MCA ($-K_1^{(2)} + K_2^{(2)}$, when $\phi = 0^\circ$) for all systems. This reveals that the in-plane dependence must be considered in the MCA calculations for these systems.

Comparing the $K_2^{(2)}$ values of the Co free standing ML with Cu, Pd, and Ag lattice constants (a_{Cu} , a_{Pd} , and a_{Ag} , respectively), we find a remarkable effect of strain on the in-plane MCA. Surprisingly, the 8% strain from a_{Cu} to a_{Pd}

TABLE I. The MCA constants, $K_1^{(2)}$ and $K_2^{(2)}$ (in meV) and magnetic moment M (in μ_B) for the free Co ML at the lattice constant corresponding to the bulk metal indicated and for Co as an overlayer on Cu(110) as substrate.

System	M	$K_1^{(2)}$	$K_2^{(2)}$
Co ML (Cu)	2.21	0.67	-0.95
Co ML (Pd)	2.25	0.74	-4.71
Co ML (Ag)	2.28	0.70	-3.60
Co overlayer(unrelaxed)/Cu(110)	1.78	-0.10	-2.56
Co overlayer(relaxed)/Cu(110)	1.65	-0.47	-2.02

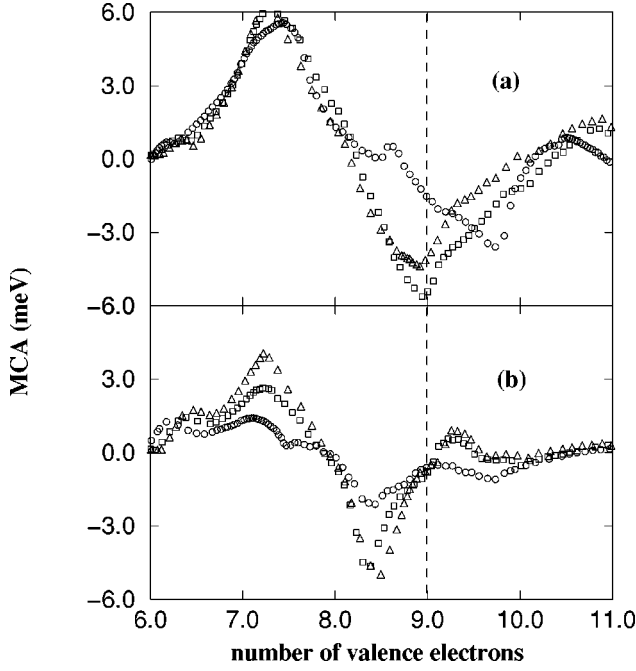


FIG. 3. Band filling dependence of MCA at (a) $\phi=0^\circ$ and (b) $\phi=90^\circ$ for monolayers with Cu (circles), Pd (squares), and Ag (triangles) lattice constants.

results in a five times larger in-plane MCA: the magnitude of $K_2^{(2)}$ increases from -0.95 to -4.71 (meV). More strain from a_{Pd} to a_{Ag} decreases the strength of the in-plane MCA to -3.60 meV, which is still almost four times larger than that of a_{Cu} . From Fig. 2, we can see that this large change of in-plane MCA is mainly due to the different influence of strain on the MCA value for different ϕ . At $\phi = 0^\circ$ the MCA values are largely changed due to the strain having the value -1.68 , -5.45 , and -4.30 meV for a_{Cu} , a_{Pd} , and a_{Ag} , respectively. As ϕ rotates to 90° , this influence is reduced and finally the MCA values for the three ML's coincide with each other at $\phi = 90^\circ$. As a result, the strength of the in-plane MCA, which can be determined roughly by the difference of MCA for $\phi = 0^\circ$ and 90° , shows a strong strain dependence.

To identify the different influence of strain for different ϕ , we plot in Fig. 3 the MCA versus band filling curves for the free standing Co ML's for $\phi = 0^\circ$ and 90° . The top panel is for $\phi = 0^\circ$ where the strain effect is maximum. The Co ML with a_{Cu} shows typical band filling behavior: positive anisotropy dominates the beginning of filling the spin-down d bands and a negative bump develops near half occupation of the bands. This MCA curve changes significantly when strain is introduced up to a_{Pd} : the peaks become sharp, and most of all, the minimum of the negative bump moves down right at the physical band filling (nine electrons). More strain (up to a_{Ag}) adds some positive contribution to the negative bump without further change in the behavior of MCA. As a result, Co ML's with a_{Pd} and a_{Ag} exhibit a large negative MCA value compared to the ML with a_{Cu} at $\phi = 0^\circ$. In contrast, for $\phi = 90^\circ$ (shown in the bottom panel), the negative peaks coincide for all ML's and the strain effect only appears in the different magnitude of the peaks. But this peak

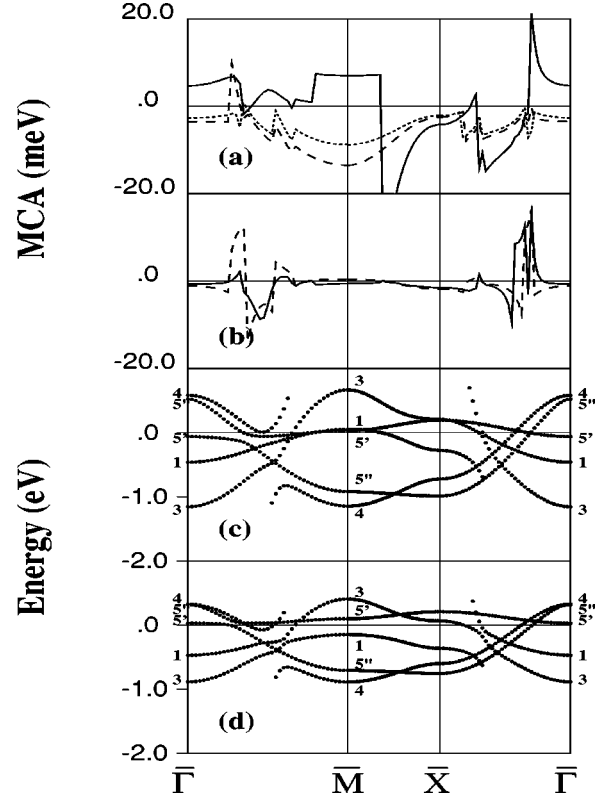


FIG. 4. Contributions to MCA for k points along the symmetry lines for free standing Co monolayers with Cu (solid), Pd (long dashed), and Ag (short dashed) lattice constants for (a) $\phi = 0^\circ$ and for (b) $\phi = 90^\circ$. Unperturbed spin-down d bands for Co with (c) Cu and (d) Pd lattice constants. Band numbers 1, 3, 4, 5', and 5'' stand for z^2 , x^2-y^2 , xy , yz , and xz orbitals, respectively. Only states with more than a 50% d component are shown.

is below the physical band filling and thus all three Co ML's exhibit the same MCA values.

The reason for the strong ϕ dependence on strain can be understood in connection with the electronic structure changes due to the strain. In Fig. 4, the contributions to MCA of each k point along the symmetry lines calculated at $\phi = 0^\circ$ and 90° are plotted together with the band plots for Co ML's with a_{Cu} and a_{Pd} [ML(a_{Cu}) and ML(a_{Pd}), respectively]. The band plots in the bottom panels show that upon introducing the 8% strain, the reduced interaction due to the increased in-plane interatomic distance results in a reduced dispersion of each band. As a result, the most significant band change occurs in broad regions around $\bar{\Gamma}$ and \bar{M} : the out of plane d_{z^2} and d_{yz} states which are both occupied (empty) at $\bar{\Gamma}$ (\bar{M}) for the ML(a_{Cu}) split into occupied and empty states for the ML(a_{Pd}). Referring to the second order perturbation applied to atomic orbitals (cf., the diatomic pair model¹⁶), the coupling between the occupied d_{z^2} state and the empty d_{yz} state (or between the empty d_{z^2} state and the occupied d_{yz} state) appears as an additional negative MCA contribution (through L_x) for $\phi = 0^\circ$ while it's contribution (through L_y) for $\phi = 90^\circ$ vanishes. Therefore the MCA for $\phi = 0^\circ$ is significantly influenced by the strain while that for $\phi = 90^\circ$ is not. This explains the difference of the strain-induced MCA change for different ϕ shown in the top panels. At $\phi = 0^\circ$ [see Fig. 4(a)], for ML(a_{Cu}) the MCA is

positive around $\bar{\Gamma}$ and \bar{M} where the d_{z^2} and d_{yz} states are both occupied or empty, while for $\text{ML}(a_{\text{Pd}})$ the negative MCA prevails in the broad regions due to the coupling between the empty d_{yz} and the occupied d_{z^2} states. But the MCA at $\phi = 90^\circ$ is less sensitive to the band change [see Fig. 4(b)]: the MCA for both ML's shows no significant difference in spite of the band change showing negligible anisotropy along the symmetry lines (except some oscillations around the k points where the bands cross near the Fermi level).

This effect does not increase monotonically, however, when we introduce more strain with the assumed Ag lattice constant: we found that the band structure for the Co ML (a_{Ag}) remains similar to that for the Co ML(a_{Pd}) but with a somewhat reduced band width. As a result, the MCA for the Co ML(a_{Ag}) in Fig. 4(a) exhibits a similar behavior to that for the Co ML(a_{Pd}) except that the magnitude of the peaks is reduced for the whole region. Without a significant band structure change, the magnitude of the crystalline anisotropy may be reduced due to the strain since the increase of the atomic distance makes the effect of directionality (crystal-field) weaker, and the environment of every atom becomes more isotropic.

Returning to the Co overlayers on Cu, the reduced surface and the presence of the nonmagnetic Cu atoms have a significant influence on the magnetic moment of Co: it is reduced to $1.78\mu_B$ for the unrelaxed overlayer, which is 20% smaller than that of the free standing Co ML (see Table I). For the relaxed overlayer, the equilibrium structure is determined by atomic force calculations in which all final \hat{z} direction forces on all atoms are negligible (< 3 mRy/a.u.) and thus the total energy reaches its minimum. Compared to the unrelaxed structure, the fully relaxed surface Co layer is found to undergo a downward relaxation by 0.62 a.u., whereas the interface Cu atom expands upward by 0.11 a.u. and the next Cu layer from the interface Cu atom contracts inward by 0.15 a.u. This relaxation of the (110) overlayer is quite large compared to the case of the (111) overlayer¹⁷ (0.30 a.u. for the Co layer). As a result, the magnetic moment of Co is reduced by $0.12\mu_B$ (see Table I), i.e., about 7% smaller than the unrelaxed case [compared to a 3% reduction for the (111) overlayer¹⁷].

By comparing the MCA of the unrelaxed Co overlayer with that of the free standing Co ML with the same lattice constant (Fig. 2), we find that a pronounced change of MCA is induced by the nonmagnetic Cu substrate. More interestingly, the effect is totally different for different ϕ : the *negative* MCA increases in magnitude by 0.84 meV at $\phi=0^\circ$ while it increases in magnitude by 0.77 meV at $\phi=90^\circ$ (and changes sign). Therefore, the strength of the in-plane MCA is changed by about three times from the value of the free ML [from -0.95 to -2.56 (meV)]. When relaxation is introduced, the MCA shifts upward from the unrelaxed case for the whole range of ϕ (see Fig. 2) — in agreement with our recent calculation for the same system in the (111) orientation, which we attributed to the increase of the interfacial hybridization due to the close interatomic distance between Co and Cu atoms.¹⁷ The strength of the in-plane MCA decreases by 20% of the value for the unrelaxed overlayer, which is also due to the different relaxation effects for dif-

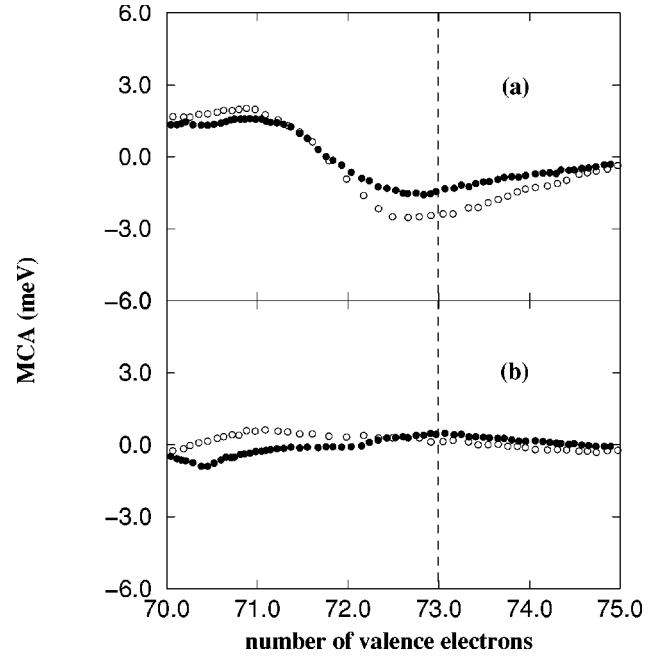


FIG. 5. Band filling dependence of MCA for Co/Cu (110) at (a) $\phi=0^\circ$ and (b) $\phi=90^\circ$ for unrelaxed (circles) and relaxed (squares) overlayers.

ferent ϕ , as can be seen from the MCA versus band filling in Fig. 5. The top panel shows a large negative peak developing around the physical filling (73 electrons) for $\phi = 0^\circ$. The relaxed overlayer has a significant positive MCA contribution developed around the physical band filling. But for $\phi = 90^\circ$, the MCA exhibits totally different behavior: any peak invoked by the change of band filling that appeared for most of the Co thin films studied previously has disappeared and the structural relaxation introduces a small positive contribution to MCA around the physical band filling. As a result, the difference of MCA for $\phi = 0^\circ$ and 90° (which gives the in-plane MCA) is reduced by the relaxation.

In conclusion, we performed first principles calculations of the interface in-plane MCA for fcc (110) Co (i) as a free standing ML with assumed Cu, Pd, and Ag lattice constants and (ii) as unrelaxed and relaxed overlayers on a Cu substrate. We found a significant in-plane MCA showing the necessity of involving the in-plane dependence in the determination of MCA for these systems. The large enhancement of the in-plane MCA by the strain is attributed to the different influence of the strain-induced change of band structure for different ϕ , where the coupling between the out of plane d states plays a crucial role. The in-plane MCA is found to be increased largely by the nonmagnetic Cu substrate, while the relaxation causes a decrease in the strength of the in-plane MCA. In spite of the large change in the strength of the in-plane MCA induced by strain or a nonmagnetic substrate, the easy axis lies along $[\bar{1}10]$, which is the direction of the in-plane nearest neighbor atoms.

This work was supported by the Office of Naval Research (Grant No.N00014-94-1-0030) and by grants of computer time at the Pittsburgh Supercomputing Center supported by the NSF Division of Advanced Scientific Computing and the Arctic Region Supercomputing Center.

- ¹G. H. O Daalderop, P. J. Kelly, M. F. H. Schuurmans, W. J. M. de Jonge, P. J. H. Bloemen and F. J. A. den Broeder, in *Ultra-thin Magnetic Structures*, edited by J. A. C. Bland and B. Heinrich (Springer, Berlin, 1994), Vol. I.
- ²P. Krams, B. Hillebrands, G. Güntherodt, and H. P. Oepen, *Phys. Rev. B* **49**, 3633 (1994).
- ³G. T. Rado, *Phys. Rev. B* **26**, 295 (1982).
- ⁴B. Heinrich and J. F. Cochran, *Adv. Phys.* **42**, 523 (1993), and references therein.
- ⁵J. G. Gay and Roy Richter, *Phys. Rev. Lett.* **56**, 2728 (1986).
- ⁶H. J. Elmers, T. Furubayashi, M. Albrecht, and U. Gradmann, *J. Appl. Phys.* **70**, 5764 (1991).
- ⁷P. Bruno, *Phys. Rev. B* **39**, 865 (1989).
- ⁸M. Cinal, D. M. Edwards, and J. Mathon, *J. Magn. Magn. Mater.* **140-144**, 681 (1995).
- ⁹J. Dorantes-Dávila and G. M. Pastor, *Phys. Rev. Lett.* **77**, 4450 (1997).
- ¹⁰R. Yu, D. Singh, and H. Krakauer, *Phys. Rev. B* **43**, 6411 (1992); R. Wu, W. Mannstadt, and A. J. Freeman (unpublished).
- ¹¹E. Wimmer, H. Krakauer, M. Weinert, and A. J. Freeman, *Phys. Rev. B* **24**, 864 (1981); M. Weinert, *J. Math. Phys.* **22**, 2433 (1981), and references therein.
- ¹²D. Koelling and B. N. Harmon, *J. Phys. C* **10**, 3107 (1977).
- ¹³H. McDonald, W. E. Pickett, and D. D. Koelling, *J. Phys. C* **13**, 2675 (1980).
- ¹⁴D. S. Wang, R. Wu, and A. J. Freeman, *Phys. Rev. Lett.* **70**, 869 (1993).
- ¹⁵X. D. Wang, R. Wu, D. S. Wang, and A. J. Freeman, *Phys. Rev. B* **54**, 61 (1996).
- ¹⁶D. S. Wang, R. Wu, and A. J. Freeman, *J. Magn. Magn. Mater.* **129**, 237 (1994).
- ¹⁷L. P. Zhong, M. Y. Kim, X. D. Wang, and A. J. Freeman, *Phys. Rev. B* **53**, 9770 (1996).